HHS Public Access

Author manuscript

J Orthop Res. Author manuscript; available in PMC 2020 September 01.

Published in final edited form as:

J Orthop Res. 2019 September ; 37(9): 1920–1928. doi:10.1002/jor.24330.

The Complex Relationship Between In Vivo ACL Elongation and Knee Kinematics During Walking and Running

Kanto Nagai, MD, PhD[1,2], **Tom Gale, MS**[1], **Daisuke Chiba, MD, PhD**[1], **Favian Su, BS**[1], **Freddie H. Fu, MD, DSc (Hon.), DPs (Hon.)**[1], **William Anderst, PhD**[1]

[1]Department of Orthopaedic Surgery, University of Pittsburgh, Pittsburgh, Pennsylvania, USA.

[2]Department of Orthopaedic Surgery, Kobe University Graduate School of Medicine, Kobe, Hyogo, Japan

Abstract

In vivo anterior cruciate ligament (ACL) bundle (anteromedial bundle [AMB] and posterolateral bundle [PLB]) relative elongation during walking and running remain unknown. In this study, we aimed to investigate *in vivo* ACL relative elongation over the full gait cycle during walking and running. Ten healthy volunteers walked and ran at a self-selected pace on an instrumented treadmill while biplane radiographs of the knee were acquired at 100Hz (walking) and 150Hz (running). Tibiofemoral kinematics were determined using a validated model-based tracking process. The boundaries of ACL insertions were identified using high-resolution MRI. The AMB and PLB centroid-to-centroid distances were calculated from the tracked bone motions, and these bundle lengths were normalized to their respective lengths on MRI to calculate relative elongation. Maximum AMB relative elongation during running (6.7 ± 2.1%) was significantly greater than walking (5.0 ± 1.7%, P = 0.043), whereas the maximum PLB relative elongation during running (1.1 ± 2.1%) was significantly smaller than walking (3.4 ± 2.3%, P = 0.014). During running, the maximum AMB relative elongation was significantly greater than the maximum PLB relative elongation (P < 0.001). ACL relative elongations were correlated with tibiofemoral six degree-of-freedom kinematics. The AMB and PLB demonstrate similar elongation patterns but different amounts of relative elongation during walking and running. The complex relationship observed between ACL relative elongation and knee kinematics indicates that ACL relative elongation is impacted by tibiofemoral kinematic parameters in addition to flexion/extension. These findings suggest that ACL strain is region-specific during walking and running.

Graphical Abstarct

This study investigated *In vivo* ACL bundle elongation over the full gait cycle during walking and running using a highly accurate biplane radiography system. The AMB and PLB demonstrate

Please address all correspondence to: William Anderst, PhD, Biodynamics Laboratory, Department of Orthopaedic Surgery, University of Pittsburgh 3820 South Water Street, Pittsburgh, PA 15203, USA anderst@pitt.edu.

Author Contribution Statement:

The co-authors and I warrant that all authors have participated in this study. Detailed contributions are as follows; Kanto Nagai (KN), Tom Gale (TG), and William Anderst (WA) conceived of the study, and all authors participated in the design of the study. KN, TG, Favian Su (FS) and WA were involved in data processing, and KN, TG, Daisuke Chiba (DC) and WA performed data analysis. All authors participated in the interpretation of the data. KN, TG, and WA wrote the manuscript, and all authors performed critical revision of the manuscript for important intellectual content. All authors have read and approved the final manuscript.

similar elongation patterns but different amounts of relative elongation during walking and running. The complex relationship observed between ACL elongation and knee kinematics indicates that ACL elongation is impacted by tibiofemoral kinematic parameters in addition to flexion/extension. These findings suggest that ACL strain is region-specific during walking and running.

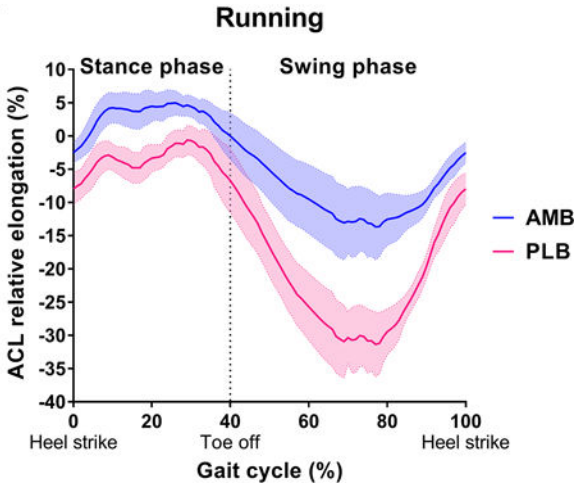

Keywords

anterior cruciate ligament; elongation; walking; running; biplane radiography system

Introduction

More than 120,000 anterior cruciate ligament (ACL) injuries occur each year in the United States.[1–3] ACL injury leads to short term disability and may result in knee articular cartilage destruction and osteoarthritis as early as 10 years after the initial injury.[4–7] Moreover, even after ACL reconstruction, tibiofemoral osteoarthritis (OA) has been detected in 41% of patients at 20-year follow-up.[8] Unfortunately, the evidence is inconclusive that ACL reconstruction decreases the long-term risk of OA.[9–11] This has led to the development of alternative reconstruction strategies, such as double-bundle ACL reconstruction.[12,13] Knowledge of how external loading and knee kinematics affect *in vivo* ACL elongation is important in order to identify mechanisms of ACL injury, improve reconstruction techniques, and design ACL injury prevention and rehabilitation protocols.[2,7,14] It is well known that the ACL is composed of two bundles: the anteromedial bundle (AMB) and the posterolateral bundle (PLB).[15,16] The function of the two bundles is often assessed in biomechanical tests that control for knee flexion angle[17]; however, biomechanical tests that do not account for the full 6 degree-of-freedom knee kinematics and loading that occurs *in vivo* may produce results that are not consistent with the *in vivo* condition. Thus, it is important to know the *in vivo* biomechanical function of the two bundles to more closely replicate the native knee function and improve surgical outcomes.

Direct measurement of *in vivo* ACL strain or elongation is challenging and has only been accomplished using an invasive procedure that required directly attaching a strain sensor to

the ACL.[18–21] A less invasive technique that has been used to estimate ACL relative elongation *in vivo* is to identify the ACL attachment points in magnetic resonance imaging (MRI) and to measure changes between attachment sites using biplane fluoroscopy.[22–24] Previous studies using this technique focused on quasi-static lunge[22,24] and slow walking[23] movements that may not replicate ACL strain during more common and dynamic activities such as walking and running. Therefore, the purpose of the present study was to investigate *in vivo* native ACL (AMB and PLB) relative elongation over the full gait cycle during walking and running using a highly accurate biplane radiography system. The hypotheses were (1) the maximum ACL bundle relative elongations would be greater during running than walking, (2) the maximum relative elongation would occur near full knee extension in the PLB and at greater knee flexion angles in the AMB, and (3) tibiofemoral kinematic parameters in addition to knee flexion angle would independently correlate with ACL relative elongation during walking and running.

Methods

Subjects

Ten healthy young adult volunteers without any report of prior knee injuries (5 male / 5 female, age: 27 ± 4 years, BMI: 24.9 ± 3.6 kg/m^2) were enrolled in this study. The subjects were non-sedentary and recruited using an online community recruitment system. The study was approved by the institutional review board and all participants provided written informed consent before enrollment.

Data collection and processing of dynamic *in vivo* kinematics

Kinematic data for ten right knees of ten participants were collected with a custom biplane radiography system as previously reported (Figure 1).[25] The participants walked and ran at a self-selected pace (1.4 ± 0.2 m/s and 2.6 ± 0.4 m/s respectively) on an instrumented treadmill (Bertec Corp, Columbus, OH), while synchronized biplane radiographs of the right knee were collected at 100 images/second (walking) for 1 second (radiographic imaging parameters: maximum 90kV, 160mA, 1ms duration pulsed exposure) and at 150 images/second (running) for 0.6 seconds. Concurrently, a 12-camera Vicon motion capture system (Vantage 5, Vicon, Oxford, UK) was used to track skin-mounted markers. Due to the limited field of view of the biplane radiography system, four trials were collected from each participant: late swing through mid-stance was imaged in the first two trials, and mid-stance through late swing was imaged in the second two trials. Each trial was normalized to percent gait cycle and the average data over all four trials were used for the analysis. Gait cycle events (heel strike and toe off) were detected using the vertical ground reaction force from the dual-belt instrumented treadmill which was recorded at 1000Hz.

Bone geometry was reconstructed from a high-resolution computed tomography (CT) scan (0.3 × 0.3 × 0.6 mm voxels). The maximum radiation exposure related to this study was estimated to be 1.26 mSv, comprised of 0.06 mSv from the CT scan and 1.2 mSv from biplane radiographic imaging (estimated using PCXMC, STUK - Radiation and Nuclear Safety Authority, Helsinki, Finland).

Anatomic coordinate systems were established for the tibia and femur by use of the subject-specific bone models.[26] Tibiofemoral motion was determined for each trial using a previously validated volumetric model-based tracking process that matches the CT bone model to the biplane radiographs.[27] The accuracy of this bone tracking system has been validated during *in vivo* running to be 0.3 ± 0.1 mm, 0.4 ± 0.2 mm, and 0.7 ± 0.2 mm in the medial-lateral, proximal-distal, and anterior-posterior directions, respectively, and to be 0.9 ± 0.3°, 0.6 ± 0.3°,and 0.3 ± 0.1° for flexion-extension, external-internal rotation, and abduction-adduction, respectively. Tibiofemoral translations and rotations were calculated as previously described.[26,28] Knee kinematic data was resampled at 1% intervals of the gait cycle. The stance phase of walking was mapped to 0% to 60% of the gait cycle and the swing phase of walking was mapped to 60% to 100% of the gait cycle for each participant. The stance phase of running was mapped to 0% to 40% of the gait cycle and the swing phase of running was mapped to 40% to 100% of the gait cycle for each participant. These ratios were determined based on the average stance-to-swing ratio of all participants.

Identification of the centroid of the AMB and PLB

The right knee of each subject was also imaged by means of a 3.0-T Magnetom Trio magnetic resonance imaging (MRI) system (Siemens) using a T2-weighted image sequence (0.35 × 0.35 × 0.70 mm; flip angle, 25°; TE, 4.7 ms; TR, 16.3 ms). The knee was fully extended during scanning. The femoral and tibial bones were segmented in the MRI images and registered to the CT-based bone models as previously described.[25] The boundaries of the femoral and tibial ACL insertions were identified using high-resolution 3T MRI with the Mimics software version 20 (Materialize, Belgium) as previously reported.[29] Briefly, the boundaries of whole femoral and tibial ACL insertions were manually identified using axial, coronal, and sagittal planes. For the identification process, the ligament-bone interface was manually marked by iteratively placing points on the insertion site boundary in each slice and adjusting placements by manually comparing to neighboring image slices.[29] A previous validation of this technique indicated that the MRI-estimated centroids of the ACL insertion were biased on average 0.6 ± 1.6 mm proximally and 0.3 ± 1.9 mm posteriorly for the femur, and 0.3 ± 1.1 mm laterally and 0.5 ± 1.5 mm anteriorly for the tibia, compared to the “gold standard” centroids measured by laser scanner.[29]

The division of AMB and PLB insertions was then performed based on previous reports on the anatomy of the ACL insertions.[15,16,30–32] The femoral ACL insertion was divided into AMB and PLB at the middle point (50/50%) of the principle long axis of whole ACL insertion using a custom MATLAB (The MathWorks, Inc. Natick, MA) code, as femoral ACL insertion was an oval shape (Figure 2A). The tibial ACL insertions were divided into AMB and PLB at the middle point (50/50%) of the projected ACL mid-substance axis (Figure 2B). The sensitivity analysis of ACL relative elongation was performed by changing the ratio of the point that divided into AMB and PLB (Supplementary Material). The validity of this technique for identifying AMB and PLB tibial insertions was confirmed using a previously reported data set.[32] The AMB and PLB centroids were positioned at the centroid of the AMB and PLB respective areas (Figure 2). The centroids of each insertion were identified and registered to the CT models using bone-to-bone registration from MRI to CT.

Calculation of the relative elongation of the ACL (AMB and PLB)

The AMB and PLB centroid-to-centroid distance was calculated from the tracked motion of the femur and tibia during walking and running. These ACL bundle lengths were normalized to their respective lengths at knee extension during MRI, which was defined as the ACL relative elongation (%) as previously described.[22–24] The relative elongation of the AMB and PLB was determined at each 1% of the gait cycle. The within-subject variability of the relative ACL elongation (%) was calculated by finding the standard deviation of the relative elongation at each percent of gait for each subject, then averaged across subjects. The maximum AMB and PLB relative elongations during walking and running were calculated for each participant, and the percent gait cycle and knee flexion angle at the maximum relative elongation was identified.

Data analysis

A paired t-test was performed to explore differences in the maximum bundle relative elongations between walking and running and between the AMB and PLB, as well as to explore the difference in the timing and knee flexion angle at the maximum relative elongation between the AMB and PLB. Normal distributions of these data were confirmed by using a Shapiro-Wilk test prior to a paired t-test. Using a sample size of ten participants, two tails, 80% power, and $\alpha = 0.05$, a paired t-test was powered to detect an effect size of Cohen d=0.99, which is a large effect. Stepwise multiple regression was performed to explore the relationship between the ACL bundle relative elongations and the 6 degree-of-freedom kinematics (Anterior [+]-Posterior [-], Lateral [+]-Medial [-], Proximal [+]-Distal [-] translation, Flexion [+]-Extension [-], Internal [+]-External [-], Abduction [+]-Adduction [-] rotation) during the stance and swing phases by using the group average data. Dependent variables were AMB and PLB relative elongations, and independent variables were the 6 degree-of-freedom kinematic variables. Fitness of the model was assessed using an adjusted R-squared. The threshold value of 10 of the variance inflation factor (VIF) was used to identify multicollinearity among the independent variables. All statistical analysis was completed using SPSS software v25.0 (IBM Corporation, Armonk, NY). Significance level was set as $P < 0.05$. Data are shown as mean ± 95% confidence interval (CI). Qualitative assessment of the relationship between ACL bundle relative elongation and knee flexion-extension angle was performed using scatter plots of the group average data.

Results

The maximum AMB relative elongation during running (6.7 ± 2.1%) was significantly greater than during walking (5.0 ± 1.7%) (P = 0.043), while the maximum PLB relative elongation during running (1.1 ± 2.1%) was significantly smaller than during walking (3.4 ± 2.3%) (P = 0.014). The AMB relative elongation had one peak, while the PLB had two peak relative elongations during the stance phase of walking and running (Figure 3).

During running, the maximum AMB relative elongation was significantly greater than the maximum PLB relative elongation (P < 0.001), while no differences were observed in the maximum AMB and PLB relative elongations during walking (P = 0.157).

The average within-subject variability in ACL relative elongation were as follows; walking, AMB = 1.4 ± 0.6%, PLB = 1.9 ± 0.8%; running, AMB = 1.7 ± 0.7%, PLB = 2.4 ± 1.0%.

During walking, the maximum AMB relative elongation occurred at 29.4 ± 12.8% of the gait cycle which corresponded to 11.3 ± 12.3° of knee flexion, and the maximum PLB relative elongation occurred at 30.9 ± 8.1% of the gait cycle which corresponded to 2.6 ± 2.9° of knee flexion. There were no significant differences observed between the peak bundle relative elongations in terms of gait cycle (P = 0.789) or knee flexion angle (P = 0.159) during walking. During running, the maximum AMB relative elongation occurred at 20.2 ± 5.4% of the gait cycle which corresponded to 29.5 ± 6.4° of knee flexion, and the maximum PLB relative elongation occurred at 20.8 ± 6.8% of the gait cycle which corresponded to 26.4 ± 7.5° of knee flexion, During running, there were no significant differences observed between the peak bundle relative elongations in terms of gait cycle (P = 0.619) or knee flexion angle (P = 0.061).

Multiple regression analysis showed that several kinematic variables were correlated to the ACL relative elongation, and these variables were different between the AMB and PLB and between the stance and swing phases (Table 1, 2). Multicollinearity was not observed in these models. A complex relationship between ACL bundle relative elongations and knee flexion angle was observed (Figure 4, 5).

Discussion

The main findings of the current study were that the patterns of the ACL bundle relative elongations over the full gait cycle and the maximum ACL relative elongation were different between walking and running, suggesting that *in vivo* ACL bundle relative elongation is dependent upon the amount of loading and loading rate, which differ between walking and running. The amount of relative elongation was different between the AMB and PLB; however, the timing of maximum AMB and PLB relative elongation was similar, suggesting regional variation exists in the ACL fiber strain during these common activities. Moreover, multiple regression analysis demonstrated a complex relationship between the ACL bundle relative elongations and knee kinematics. Several kinematic parameters provided unique information to improve prediction of the complex *in vivo* relative elongation pattern of the ACL during walking and running. Limitations of predicting ACL relative elongation from flexion angle alone are demonstrated in Figures 4A and 5A which clearly show three different relative elongations of the AMB at 15° of knee flexion during walking and at 36° of flexion during running. These results demonstrate the influence of internal (muscular) and external (ground reaction force) loading on ACL relative elongation *in vivo*.

The continuous AMB and PLB relative elongation curves provide novel information related to ACL function *in vivo*. As expected, the AMB and PLB relative elongations were greater during the stance phase in comparison to swing, and there was a very well-defined peak soon after heel strike (Figure 3). The PLB relative elongation curve demonstrated a second clear peak during the push-off phase of walking, suggesting a strong relationship between PLB relative elongation and knee extension during push-off. Although the relative elongation patterns were similar in the AMB and PLB, differences in relative elongation of

the bundles were observed. Previously observed differences in material and microstructural properties of the AMB and PLB during loading[33] may be an adaptation to relative elongation differences observed in this study. These observed differences in relative strain suggest non-uniform loading of the fibers of the ACL. In terms of ACL reconstruction, it is not clear if two bundles are necessary or if a single bundle with varying properties would suffice to replicate this native ACL function. Although the AMB relative elongation was greater than PLB relative elongation over the full gait cycle in the present study, it should be noted that the ACL length during the motion was normalized by the bundle length during MRI, therefore absolute elongations in each bundle could not be determined.[22–24]

The maximum AMB relative elongation was significantly greater during running than walking, supporting the first hypothesis. On the other hand, the maximum PLB relative elongation was greater during walking than running, which was contrary to the first hypothesis. As shown in Figure 4C and 5C, the knee achieved greater extension during walking than running. Previous cadaveric studies have shown that the PLB was taut near full knee extension and relaxed rapidly as the knee flexed.[17] Those findings suggest that the difference in the maximum PLB relative elongation observed in this study was partially attributable to differences in maximum knee extension during the two activities. In the current study, although there were no significant differences in timing or knee flexion angle at maximum relative elongation of the AMB and PLB bundles, it is worth noting that there was large variability among subjects in timing and knee flexion angle at the maximum ACL bundle relative elongation. The current findings suggest that *in vivo* functions of the AMB and PLB may be more synergistic rather than reciprocal which was observed by the previous biomechanical studies using cadaveric knees.[17,34–36] These current findings are supported by the previous studies of *in vivo* ACL relative elongation during quasi-static lunge[22,24] and walking.[23] This inconsistency between *in vivo* and *in vitro* may be because *in vitro* biomechanical tests do not account for the full 6 degree-of-freedom knee kinematics and loading that occurs *in vivo*.

In vivo ACL elongation or strain has been previously investigated during relatively low-impact activities such as knee flexion-extension,[18,21] squatting,[18] bicycling,[20] and quasi-static lunge,[22,24] with inconsistent results reported among studies that directly measured or indirectly calculated ACL strain. In a series of studies, Beynnon and colleagues arthroscopically implanted a differential variable reluctance transducer onto the ACL.[18–21] These studies reported ACL strain was highest near full knee extension, with peak values between 0% and 4% depending on the movement.[19] Three previous studies reported *in vivo* ACL relative elongation during walking.[23,37,38] Shelburne et al.[38] reported ACL forces during gait by using a musculoskeletal model of the knee. Their ACL force pattern showed a steep rise from foot strike to 15% of the gait cycle, in agreement with the present data indicating an increase in ACL length during the impact phase of gait. On the other hand, Wu et al.[23] calculated AMB and PLB relative elongation during the stance phase of unnaturally slow gait (0.67 m/s) and reported that AMB and PLB lengths decreased during the loading response phase and peaked during midstance at 12% and 13%, respectively. Taylor et al.[37] also reported the maximum ACL relative elongation (13%) occurred near the maximum knee extension during the midstance to terminal stance phase of gait; however, as a limitation, only a skin-mounted marker system was used for the data collection during

walking, which is known to be prone to errors as large as 16.1 mm and 13.1° due to relative motion between the markers and underlying bones.[39,40] Possible explanations for differences in estimated ACL relative elongation during the loading response phase include the abnormally slow gait in the study by Wu et al.[23], resulting in less impact loading, and the use of skin-mounted markers in the study by Taylor et al.[37] Differences in the magnitude of relative ACL strain may be related to differences in ACL length during the MRI.

The average within-subject variability in ACL bundle relative elongation was within 1.5% to 2.5 % over the entire gait cycle in the present study. Increasing the number of movement trials may provide a more accurate assessment of within-subject variability in ACL relative elongation. To best of our knowledge, no previous research reports the variability in relative elongation of the ACL, and there is a clear need for further research to characterize the envelope of function for the ACL during dynamic activities.

The stepwise multiple regression was valuable for identifying kinematic variables related to the relative elongation of AMB and PLB during walking and running. The present results showed that not only knee flexion-extension but also anterior-posterior translation was strongly correlated to the ACL bundle elongation during the stance phase, but not the swing phase (Table 1, 2). The complex relative elongation pattern of the ACL bundles is highlighted by the fact that different kinematic variables were correlated with the ACL bundle relative elongation, and these differences were not only between the stance and swing phases, but also between AMB and PLB as well as between walking and running. Previous reports showed the inverse linear relationship between knee flexion angle and ACL strain/elongation during active knee extension-flexion,[18] squatting,[18] and slow walking.[23] However, their relationship during more dynamic activities such as walking and running have not been reported. In the present study, the scatter plots of the average knee flexion angle versus ACL bundle relative elongations demonstrated a complex relationship, especially during the stance phase of walking and running (Figure 4, 5). These quantitative findings demonstrate the significant role loading plays in ACL relative elongation *in vivo* during dynamic activities. This finding emphasizes the importance of reproducing the *in vivo* loading condition when performing ACL-related cadaveric studies. Finally, the correlational analysis demonstrates that computational models of the knee that directly link ACL elongation to knee flexion angle can be improved by including additional kinematics parameters to predict ACL elongation.

Some limitations in the present study should be noted. First, the small sample size may have precluded identifying some true differences; however, in spite of the small sample size, significant differences between walking and running and between AMB and PLB were identified in the present study. Moreover, the sample size in the current study is similar in size to most previous studies that investigated *in vivo* ACL strain or elongation.[18,20,21,23,37] Second, due to the inability to differentiate AMB and PLB insertions on MRI, the insertion sites were calculated according previous reports on the anatomy of the ACL insertions and validated using a previously reported data set.[32] A third limitation is that the ACL length was normalized by the length at static knee full extension during MRI; thus only relative ACL elongations could be determined. However, this is the common method used to estimate in vivo ligament elongation during dynamic activities,[22–24] and, to the best of our

knowledge, no technique has been developed to non-invasively determine the resting length of the ACL bundles in humans (the length of the taut-slack transition). Fourth, the results reported here are limited to straight-ahead movements of walking and running and should not be extrapolated to apply to cutting or pivoting motions. Finally, the generalizability of the present study is limited, as different ethnic groups, the effects of age and fatigue, or other potential factors were not tested.

Conclusion

In vivo ACL bundle relative elongations are dependent upon the activity, and the relative elongation of the AMB and PLB are different and correlated to not only knee flexion angle but also other kinematic variables such as anterior tibial translation. The relative elongation patterns of the AMB and PLB suggests that the ACL experiences regional strain differences during walking and running. The current novel findings are valuable for improving ACL reconstruction, for improving injury prevention and rehabilitation protocols, and for improving the biofidelity of biomechanical and computational models of the knee.

Supplementary Material

Refer to Web version on PubMed Central for supplementary material.

Acknowledgements

This research was funded by the National Institute of Health, United States. Grant # 2R44HD066831–02A1.

References

1. Frank CB, Jackson DW. 1997 Current Concepts Review - The Science of Reconstruction of the Anterior Cruciate Ligament. J Bone Joint Surg Am 79:1556–1576. [PubMed: 9378743]
2. Hewett TE, Di Stasi SL, Myer GD. 2013 Current concepts for injury prevention in athletes after anterior cruciate ligament reconstruction. Am J Sports Med 41:216–224. [PubMed: 23041233]
3. Dodwell ER, Lamont LE, Green DW, et al. 2014 20 years of pediatric anterior cruciate ligament reconstruction in New York state. Am J Sports Med 42:675–680. [PubMed: 24477820]
4. Lohmander LS, Englund PM, Dahl LL, Roos EM. 2007 The long-term consequence of anterior cruciate ligament and meniscus injuries: Osteoarthritis. Am J Sports Med 35:1756–1769. [PubMed: 17761605]
5. Gelber AC, Hochberg MC, Mead LA, et al. 2000 Joint injury in young adults and risk for subsequent knee and hip osteoarthritis. Ann Intern Med 133:321–8. [PubMed: 10979876]
6. Myklebust G, Bahr R. 2005 Return to play guidelines after anterior cruciate ligament surgery. Br J Sports Med 39:127–31. [PubMed: 15728687]
7. Hewett TE, Myer GD, Ford KR, et al. 2016 Mechanisms, prediction, and prevention of ACL injuries: Cut risk with three sharpened and validated tools. J Orthop Res 34:1843–1855. [PubMed: 27612195]
8. Risberg MA, Oiestad BE, Gunderson R, et al. 2016 Changes in Knee Osteoarthritis, Symptoms, and Function After Anterior Cruciate Ligament Reconstruction. Am J Sports Med 44:1215–1224. [PubMed: 26912282]
9. Frobell RB, Le Graverand MP, Buck R, et al. 2009 The acutely ACL injured knee assessed by MRI: changes in joint fluid, bone marrow lesions, and cartilage during the first year. Osteoarthritis Cartilage 17:161–167. [PubMed: 18760637]
10. Frobell RB, Roos EM, Roos HP, et al. 2010 A Randomized Trial of Treatment for Acute Anterior Cruciate Ligament Tears. N Engl J Med 363:331–342. [PubMed: 20660401]

11. Frobell RB, Roos HP, Roos EM, et al. 2013 Treatment for acute anterior cruciate ligament tear: five year outcome of randomised trial. Bmj 346:f232. [PubMed: 23349407]
12. Araki D, Kuroda R, Kubo S, et al. 2011 A prospective randomised study of anatomical single-bundle versus double-bundle anterior cruciate ligament reconstruction: Quantitative evaluation using an electromagnetic measurement system. Int Orthop 35:439–446. [PubMed: 20734043]
13. Hussein M, Van Eck CF, Cretnik A, et al. 2012 Prospective randomized clinical evaluation of conventional single-bundle, anatomic single-bundle, and anatomic double-bundle anterior cruciate ligament reconstruction: 281 cases with 3- to 5-year follow-up. Am J Sports Med 40:512–520. [PubMed: 22085729]
14. Bates NA, Schilaty ND, Nagelli C V., et al. 2018 Validation of Noncontact Anterior Cruciate Ligament Tears Produced by a Mechanical Impact Simulator Against the Clinical Presentation of Injury. Am J Sports Med 46:2113–2121. [PubMed: 29864374]
15. Kopf S, Musahl V, Tashman S, et al. 2009 A systematic review of the femoral origin and tibial insertion morphology of the ACL. Knee Surg Sport Traumatol Arthrosc 17:213–219.
16. Hara K, Mochizuki T, Sekiya I, et al. 2009 Anatomy of Normal Human Anterior Cruciate Ligament Attachments Evaluated by Divided Small Bundles. Am J Sports Med 37:2386–2391. [PubMed: 19940312]
17. Amis AA. 2012 The functions of the fibre bundles of the anterior cruciate ligament in anterior drawer, rotational laxity and the pivot shift. Knee Surg Sport Traumatol Arthrosc 20:613–620.
18. Beynnon BD, Johnson RJ, Fleming BC, et al. 1997 The Strain Behavior of the Anterior Cruciate Ligament During Squatting and Active Flexion-Extension. Am J Sports Med 25:823–829. [PubMed: 9397272]
19. Beynnon BD, Fleming BC. 1998 Anterior Cruciate Ligament Strain in-Vivo: a Review of Previous Work. J Biomech 31:519–525. [PubMed: 9755036]
20. Fleming BC, Beynnon BD, Renstrom P a, et al. 1998 The Strain Behavior of the Anterior Cruciate Ligament During Bicycling. Am J Sports Med 26:109–118. [PubMed: 9474411]
21. Beynnon BD, Fleming BC, Johnson RJ, et al. 1995 Anterior cruciate ligament strain behavior during rehabilitation exercises in vivo. Am J Sports Med 23:24–34. [PubMed: 7726347]
22. Li G, DeFrate LE, Sun H, Gill TJ. 2004 In Vivo Elongation of the Anterior Cruciate Ligament and Posterior Cruciate Ligament during Knee Flexion. Am J Sports Med 32:1415–1420. [PubMed: 15310565]
23. Wu J-L, Hosseini A, Kozanek M, et al. 2010 Kinematics of the anterior cruciate ligament during gait. Am J Sports Med 38:1475–82. [PubMed: 20442323]
24. Jordan SS, DeFrate LE, Kyung Wook Nha, et al. 2007 The In Vivo Kinematics of the Anteromedial and Posterolateral Bundles of the Anterior Cruciate Ligament During Weightbearing Knee Flexion. Am J Sports Med 35:547–554. [PubMed: 17261571]
25. Nagai K, Gale T, Irrgang JJ, et al. 2018 Anterior Cruciate Ligament Reconstruction Affects Tibiofemoral Joint Congruency During Dynamic Functional Movement. Am J Sports Med 46:1566–1574. [PubMed: 29613816]
26. Tashman S, Anderst W, Kolowich P, et al. 2004 Kinematics of the ACL-deficient canine knee during gait: Serial changes over two years. J Orthop Res 22:931–941. [PubMed: 15304262]
27. Anderst W, Zauel R, Bishop J, et al. 2009 Validation of three-dimensional model-based tibio-femoral tracking during running. Med Eng Phys 31:10–16. [PubMed: 18434230]
28. Tashman S, Kolowich P, Collon D, et al. 2007 Dynamic Function of the ACL-reconstructed Knee during Running. Clin Orthop Relat Res 454:66–73. [PubMed: 17091011]
29. Araki D, Thorhauer E, Tashman S. 2018 Three-dimensional isotropic magnetic resonance imaging can provide a reliable estimate of the native anterior cruciate ligament insertion site anatomy. Knee Surg Sport Traumatol Arthrosc 26:1311–1318.
30. Ferretti M, Ekdahl M, Shen W, Fu FH. 2007 Osseous Landmarks of the Femoral Attachment of the Anterior Cruciate Ligament: An Anatomic Study. Arthroscopy 23:1218–1225. [PubMed: 17986410]
31. Ferretti M, Levicoff EA, Macpherson TA, et al. 2007 The Fetal Anterior Cruciate Ligament: An Anatomic and Histologic Study. Arthroscopy 23:278–283. [PubMed: 17349471]

32. Tashiro Y, Lucidi GA, Gale T, et al. 2018 Anterior cruciate ligament tibial insertion site is elliptical or triangular shaped in healthy young adults: high-resolution 3-T MRI analysis. Knee Surg Sport Traumatol Arthrosc 26:485–490.

33. Skelley NW, Castile RM, York TE, et al. 2015 Differences in the microstructural properties of the anteromedial and posterolateral bundles of the anterior cruciate ligament. Am J Sports Med 43:928–936. [PubMed: 25634908]

34. Kurosawa H, Yamakoshi K, Yasuda K, Sasaki T. 1991 Simultaneous measurement of changes in length of the cruciate ligaments during knee motion. Clin Orthop Relat Res :233–40.

35. Gabriel MT, Wong EK, Woo SLY, et al. 2004 Distribution of in situ forces in the anterior cruciate ligament in response to rotatory loads. J Orthop Res 22:85–89. [PubMed: 14656664]

36. Amis AA, Dawkins GP. 1991 Functional anatomy of the anterior cruciate ligament. Fibre bundle actions related to ligament replacements and injuries. J Bone Joint Surg Br 73:260–7. [PubMed: 2005151]

37. Taylor KA, Cutcliffe HC, Queen RM, et al. 2013 In vivo measurement of ACL length and relative strain during walking. J Biomech 46:478–483. [PubMed: 23178040]

38. Shelburne KB, Pandy MG, Anderson FC, Torry MR. 2004 Pattern of anterior cruciate ligament force in normal walking. J Biomech 37:797–805. [PubMed: 15111067]

39. Benoit DL, Ramsey DK, Lamontagne M, et al. 2006 Effect of skin movement artifact on knee kinematics during gait and cutting motions measured in vivo. Gait Posture 24:152–164. [PubMed: 16260140]

40. Li K, Zheng L, Tashman S, Zhang X. 2012 The inaccuracy of surface-measured model-derived tibiofemoral kinematics. J Biomech 45:2719–2723. [PubMed: 22964018]

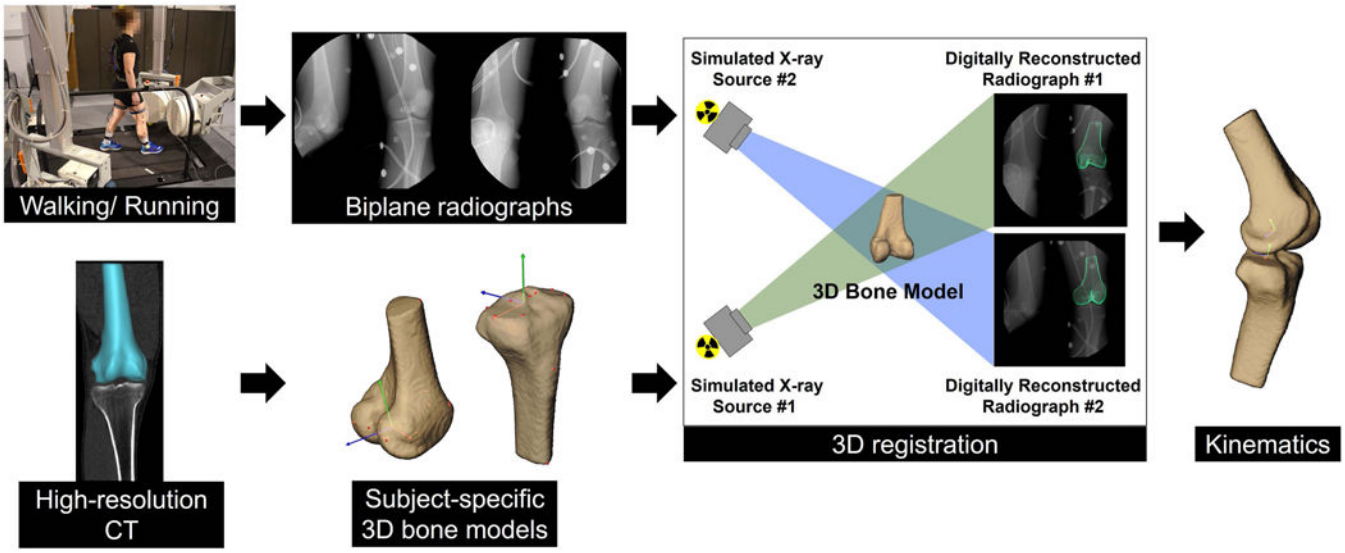

Figure 1. Data collection and processing using the biplane radiography system.

Two sets of radiographic generators, image intensifiers and high-speed digital video cameras simultaneously acquired dynamic radiographic images during level walking and running on an instrumented treadmill. Biplane radiographs and subject-specific 3D bone models, obtained from high-resolution computed tomography, were registered using a previously validated model-based tracking process to determine tibiofemoral kinematics.

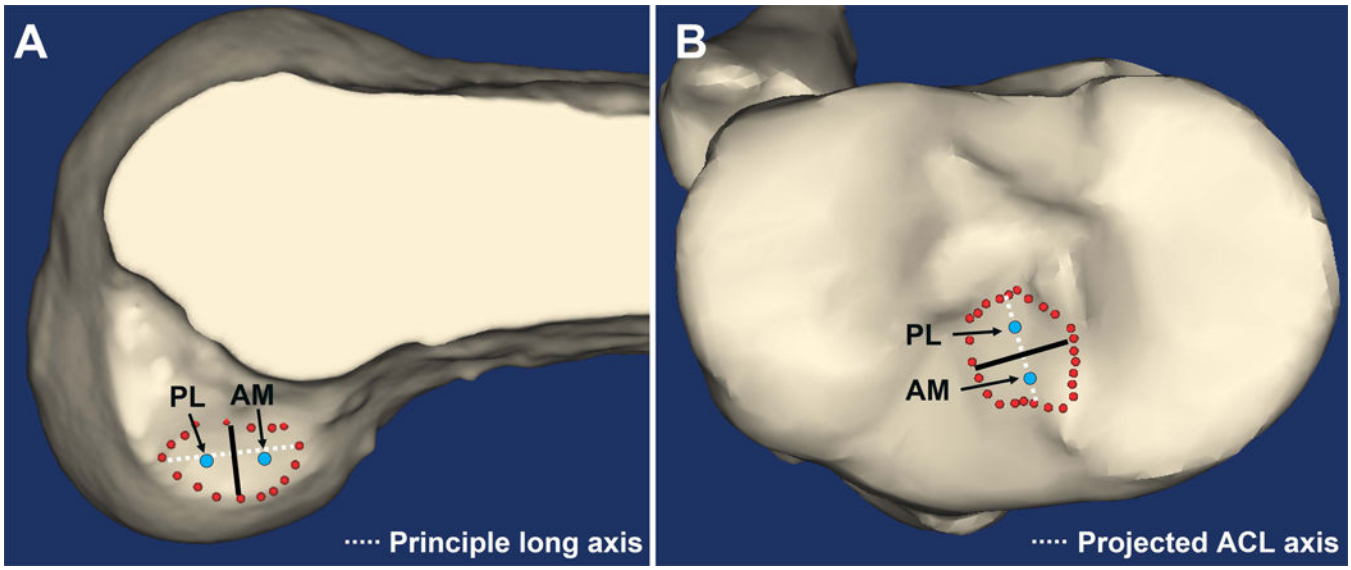

Figure 2. Representation of the ACL insertions division into two bundles

(A) Femoral and (B) tibial ACL insertions. The red dots indicate the boundaries of whole ACL insertions, and the blue dots indicate the centroids of the insertions of AM and PL bundles of the right knee. White dotted lines indicate the principle long axis on femur and the projected ACL axis on tibia, respectively. Black lines are the calculated borders of AM and PL bundles. AM: anteromedial, PL: posterolateral

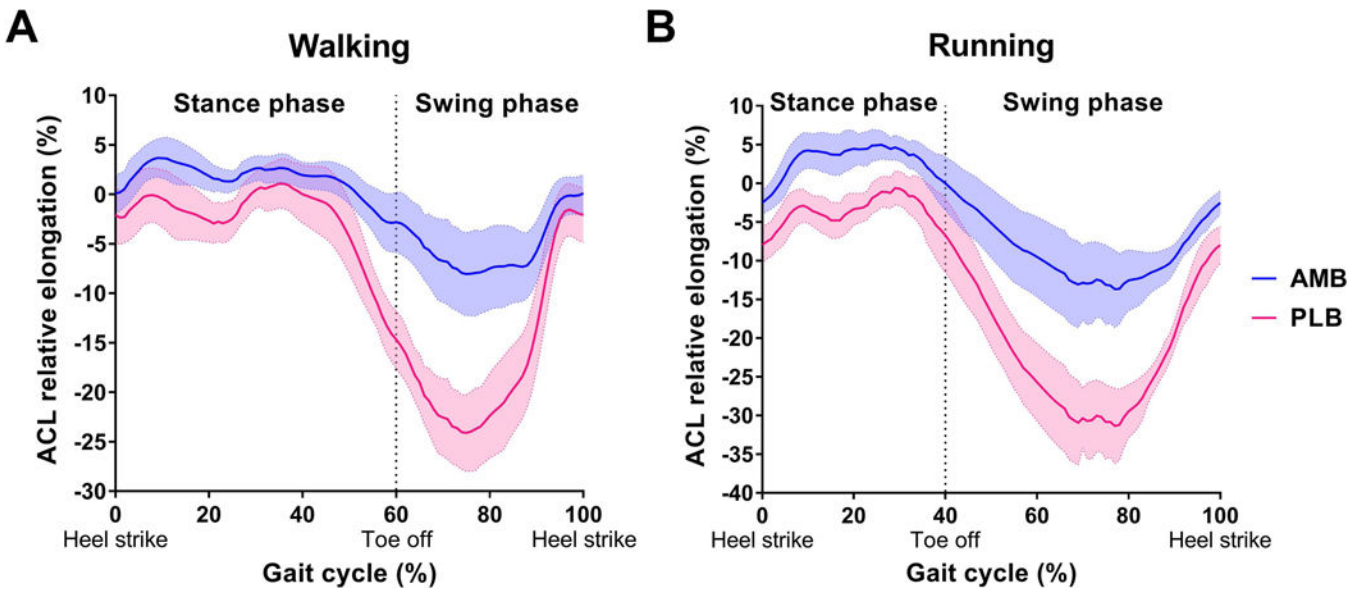

Figure 3. ACL relative elongation during walking and running.

The blue and pink lines indicate the mean AMB and PLB relative elongation, respectively, for the entire group of participants. Shaded area indicates 95% confidence interval. AMB: anteromedial bundle, PLB: posterolateral bundle

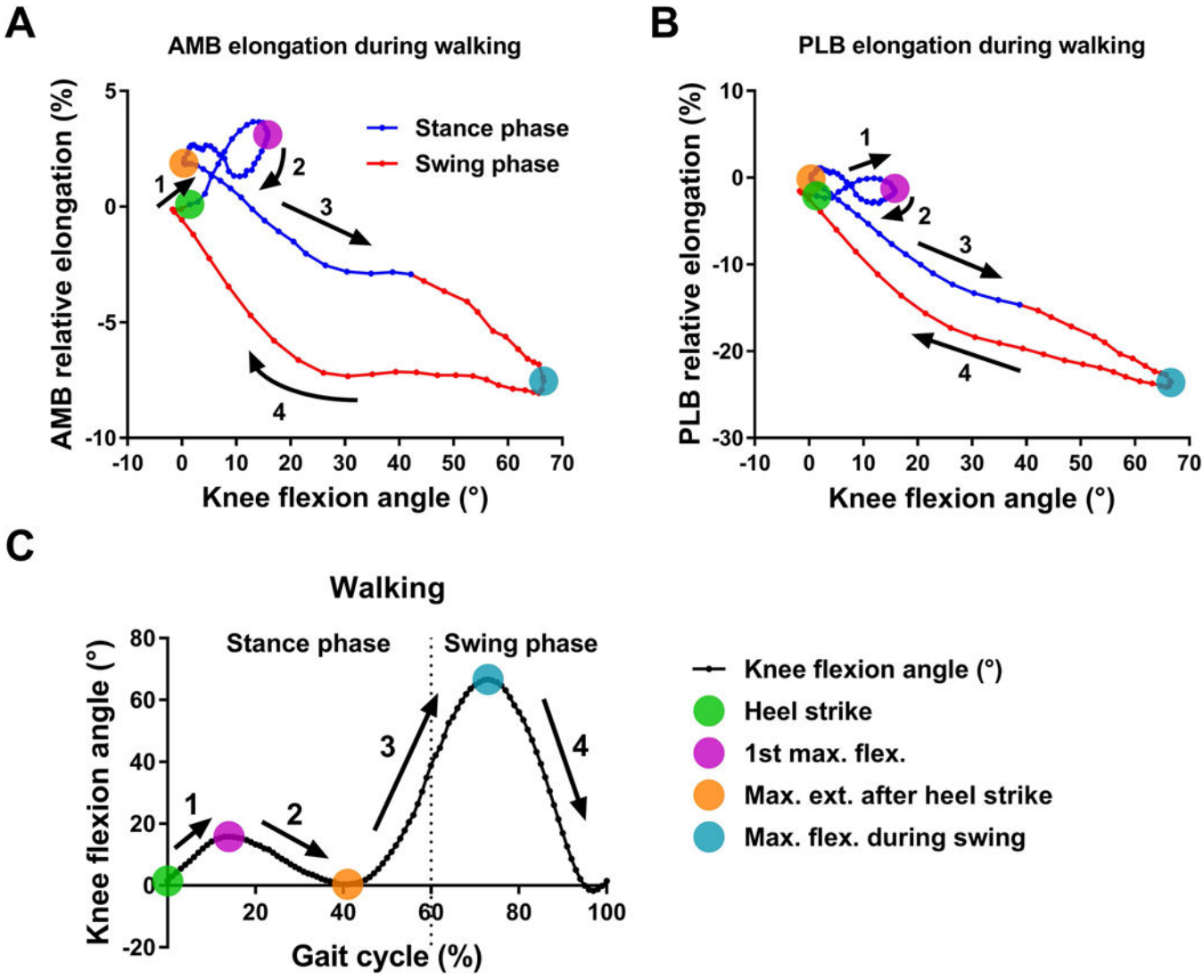

Figure 4. The complex relationship between the ACL bundle elongation and knee flexion angle during walking.

Scatter plots of the average data of (A) AMB and (B) PLB elongation versus knee flexion angle during walking. (C) The average data of knee flexion angle over the full gait cycle during walking. The four colored dots indicate key gait cycle instants. The numbers and arrows correspond to gait phases between key instants of the gait cycle.

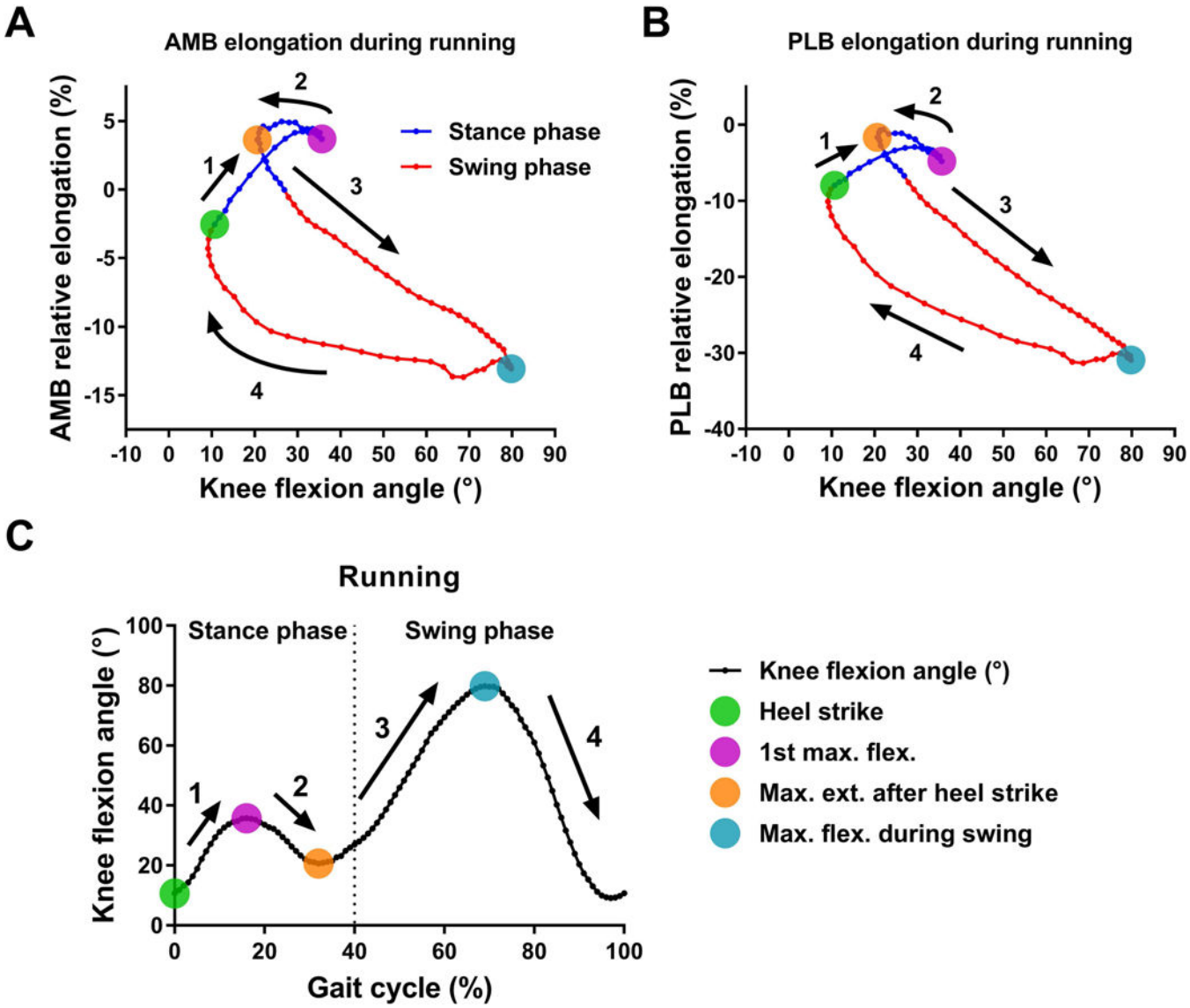

Figure 5. The complex relationship between ACL bundle elongation and knee flexion angle during running

Scatter plots of the average data of (A) AMB and (B) PLB elongation versus knee flexion angle during running. (C) The average data of knee flexion angle over the full gait cycle during running. The four colored dots indicate key gait cycle instants. The numbers and arrows correspond to gait phases between key instants of the gait cycle.

Table 1.

Multiple regression analysis identifying kinematic variables associated with AMB and PLB relative elongation during walking.

AMB elongation									
Stance phase					**Swing phase**				
Model	**B**	***SE* B**	**β**	***P* value**	**Model**	**B**	***SE* B**	**β**	***P* value**
(Constant)	−20.07	4.977			(Constant)	−0.387	0.306		
Anterior-Posterior	1.821	0.072	0.882	< 0.001	Lateral-Medial	−1.403	0.108	0.977	< 0.001
Flexion-Extension	−0.118	0.01	−0.590	< 0.001					
Proximal-Distal	−0.465	0.182	−0.158	0.013					
R^2 = 0.976, ANOVA *P* < 0.001					R^2 = 0.953, ANOVA *P* < 0.001				
PLB elongation									
Stance phase					**Swing phase**				
Model	**B**	***SE* B**	**β**	***P* value**	**Model**	**B**	***SE* B**	**β**	***P* value**
(Constant)	−12.167	0.571			(Constant)	−183.696	27.028		
Flexion-Extension	−0.342	0.014	−0.739	< 0.001	Proximal-Distal	−7.044	1.063	−0.566	< 0.001
Anterior-Posterior	2.197	0.095	0.458	< 0.001	Flexion-Extension	−0.136	0.027	−0.433	< 0.001
Internal-External	−0.363	0.050	−0.223	< 0.001					
R^2 = 0.981, ANOVA *P* < 0.001					R^2 = 0.957, ANOVA *P* < 0.001				

B, unstandardized coefficients; β, the standardized coefficients; *SE*, standard error

Table 2.

Multiple regression analysis identifying kinematic variables associated with AMB and PLB relative elongation during running.

AMB elongation									
Stance phase					**Swing phase**				
Model	**B**	***SE* B**	**β**	***P* value**	**Model**	**B**	***SE* B**	**β**	***P* value**
(Constant)	−10.422	0.472			(Constant)	12.593	0.889		
Anterior-Posterior	2.320	0.114	1.536	< 0.001	Abduction-Adduction	4.177	0.220	0.825	< 0.001
Flexion-Extension	−0.197	0.022	−0.673	< 0.001	Flexion-Extension	−0.035	0.007	−0.214	< 0.001
R^2 = 0.956, ANOVA *P* < 0.001					R^2 = 0.925, ANOVA *P* < 0.001				
PLB elongation									
Stance phase					**Swing phase**				
Model	**B**	***SE* B**	**β**	***P* value**	**Model**	**B**	***SE* B**	**β**	***P* value**
(Constant)	−24.004	0.787			(Constant)	15.341	1.161		
Anterior-Posterior	2.414	0.079	1.716	< 0.001	Abduction-Adduction	6.173	0.287	0.603	< 0.001
Flexion-Extension	−0.345	0.014	−1.324	< 0.001	Flexion-Extension	−0.167	0.009	−0.507	< 0.001
Lateral-Medial	2.959	0.267	0.276	< 0.001					
R^2 = 0.986, ANOVA *P* < 0.001					R^2 = 0.969, ANOVA *P* < 0.001				

B, unstandardized coefficients; β, the standardized coefficients; *SE*, standard error